HHS Public Access

Author manuscript

*Mol Cell*. Author manuscript; available in PMC 2018 September 21.

Published in final edited form as:

*Mol Cell*. 2017 September 21; 67(6): 962–973.e5. doi:10.1016/j.molcel.2017.08.012.

# Endoplasmic reticulum transport of glutathione by Sec61 is regulated by Ero1 and Bip

**Alise Ponsero**[1,#], **Aeid Igbaria**[1,4,#], **Maxwell A. Darch**[2], **Samia Miled**[1], **Caryn E. Outten**[2], **Jakob R. Winther**[3], **Gael Palais**[1], **Benoit D'autreaux**[1], **Agnes Delaunay-Moisan**[1], and **Michel B. Toledano**[1,*]

[1]Institute for Integrative Biology of the Cell (I2BC), CNRS, CEA–Saclay, Université Paris–Saclay, iBiTecS/SBIGEM, Laboratoire Stress Oxydant et Cancer, Gif-sur-Yvette, France

[2]University of South Carolina, Department of Chemistry and Biochemistry, Columbia, SC 29208 USA

[3]Department of Biology, University of Copenhagen, DK-2200 Copenhagen N, Denmark

## Abstract

In the endoplasmic reticulum (ER), Ero1 catalyzes disulfide bond formation and promotes glutathione (GSH) oxidation to GSSG. Since glutathione cannot be reduced in the ER, maintenance of the ER GSH redox state and levels likely depend on ER GSH import and GSSG export. We used quantitative GSH and GSSG biosensors to monitor GSH import into the ER of yeast cells. We found that GSH enters the ER by facilitated diffusion through the Sec61 protein-conducting channel, while oxidized Bip (Kar2) inhibits transport. Increased ER GSH import triggers $H_2O_2$-dependent Bip oxidation through Ero1 reductive activation, which inhibits GSH import in a negative regulatory loop. During ER stress, transport is activated by UPR-dependent Ero1 induction and cytosolic GSH levels increase. Thus, the ER redox poise is tuned by reciprocal control of GSH import and Ero1 activation. The ER protein-conducting channel is thus permeable to small molecules, provided the driving force of a concentration gradient.

### Keywords

Glutathione; Ero1; Sec61; Bip; endoplasmic reticulum; membrane transport; oxidative protein folding

## Introduction

The small thiol glutathione (GSH) is a ubiquitous nucleophile and cellular thiol-reducing buffer by virtue of its abundance. Together with glutaredoxins, GSH acts to reduce disulfide

*Correspondence: michel.toledano@cea.fr.

[4]Present address: Department of Medicine, University of California, San Francisco, San Francisco, CA 94143, USA

[#]These authors contributed equally to the work

**Authors contributions**

MBT, CEO, ADM, BdA and JRW conceived and designed the experiments. MBT wrote the manuscript. AP, AI, MD, and SM performed the experiments.

bonds, and is in turn oxidized to glutathione disulfide (GSSG), which is reduced by NADPH-dependent glutathione reductase (Toledano et al., 2007). In *S. cerevisiae*, both GSH biosynthesis and degradation take place in the cytosol, while glutathione reductase is only present in the cytosol and mitochondrial matrix (Toledano et al., 2007). Thus, GSH:GSSG pools in the other cell compartments are insulated from systems that govern GSH homeostasis. In these compartments, GSH:GSSG pools adopt very different redox potentials ($E_{GSH}$) that vary from −289 mV in the cytosol (Ostergaard et al., 2004) to −240 mV in the endoplasmic reticulum (ER) (Delic et al., 2010). These subcellular differences presumably reflect differences in GSH redox functions and suggest the need for regulated fluxes of GSH and GSSG between the cytosol and these compartments to maintain subcellular GSH homeostasis.

The ER offers a unique setting with regard to GSH homeostasis. It contains the thiol oxidase Ero1, which catalyzes the formation of disulfides transmitted to folding substrates via protein disulfide isomerase (Pdi1) (Frand and Kaiser, 1999; Pollard et al., 1998). Ero1 is itself negatively feedback regulated by regulatory disulfides that are thought to form when the ER become too oxidized (Sevier et al., 2007). A net ER reducing power is also required by Pdi1 for isomerization of these disulfides into their native arrangement, and for reduction of terminally misfolded proteins before retrotranslocation (Margittai and Sitia, 2011). In the ER, GSH is suspected of providing this reducing power (Chakravarthi and Bulleid, 2004; Cuozzo and Kaiser, 1999; Molteni et al., 2004). Since GSH is oxidized but not reduced in the ER, GSH must be imported into the ER, while GSSG is exported to the cytosol. Further, as GSH paradoxically promotes ER oxidation by Ero1 reductive activation (Kumar et al., 2011), the GSH and GSSG ER-to-cytosol fluxes must be regulated to maintain the ER redox poise.

We have addressed here the mechanism of GSH trafficking into the ER of *S. cerevisiae*. We found that the ER import of GSH occurs by facilitated diffusion through the ER Sec61 protein-conducting channel, and is regulated by the ER Hsp70 Kar2 (Bip). We also found that GSH transport is stimulated by ER stress through increases of the levels of both Ero1, which are set by the unfolded protein response (UPR), and cellular GSH. Based on these data, we propose a model establishing reciprocal control between the ER import of GSH and Ero1 activation, which functions to maintain ER redox poise. These data also suggest that the ER protein-conducting channel is generally permeable to small molecules.

## Results

### 1. The concentration of GSH in the ER and cytosol is equal

To monitor GSH fluxes across the ER membrane, we accessed its absolute concentration in the cytosol ($[GSx]_{Cyt}$) and ER ($[GSx]_{ER}$), with the use of two distinct GSH biosensors (Montero et al., 2013). The dithiol yellow-fluorescent protein (YFP)-based GSH biosensor (rxYFP) equilibrates with GSH in a manner proportional to the $[GSH]^2/[GSSG]$ ratio (Ostergaard et al., 2004). The second sensor is 1-Cys-Grx1, a mutant of glutaredoxin 1 (Grx1) with a Cys to Ser substitution of its resolving cysteine that equilibrates in a manner proportional to the GSH/GSSG ratio (Iversen et al., 2010). The concentration of GSx ([GSx] = [GSH] + 2[GSSG]) is calculated from the experimental values obtained with the two

probes (see Fig. 1D, Fig. 2D, supplemental methods). Probes were expressed in the cytosol with no targeting signals, and in the ER by insertion of the Mns1-signal peptide at the N-terminus and ER retrieval HDEL motif at the C-terminus (ER-rxYFP, ER-1-Cys-Grx1). Proper ER localization was verified by fluorescence microscopy and cell fractionation (Fig. S1). The 1-Cys-Grx1 probe relies on formation of a mixed disulfide between the enzyme and GSH. However, due to the highly reducing nature of the wild type (Wt) cytosol, this disulfide cannot form, thus preventing measurement of $[GSx]_{Cyt}$. We instead used a strain lacking glutathione reductase (Δ*glr1*) that has a more oxidizing cytosol (Hu et al., 2008), which allowed measuring a $[GSx]_{Cyt}$ value of 31.1 mM (Table 1). Although this concentration is 4.5-fold higher than the GSx value (7.14 ± 1.0 mM) estimated by enzyme assay of whole lysates from the same cells ($[GSx]_{TotCell}$), it is compatible with estimates of the yeast cytosolic distribution volume to account for 20–30 % of the total cell volume. We thus used in this study the 4.5-fold corrected value of $[GSx]_{TotCell}$ as a proxy of $[GSx]_{Cyt}$ ($[GSx]_{Corr.Cyt}$) in Wt cells. Note that as measured in Δ*glr1*, $[GSSG]_{Corr.Cyt}$ is higher than $[GSSG]_{Cyt}$ (1.83 ± 0.23 *vs.* 0.50 ± 0.03 mM) as it includes a vacuolar pool of GSSG (Morgan et al., 2013), hence precluding application of the $[GSx]_{TotCell}$ correction to [GSSG]. Table 1 compares the measured GSH parameters in the ER and cytosol of Wt and Δ*glr1*. In the cytosol, $E_{GSH}$ was more oxidizing in Δ*glr1* than in Wt (−246 ± 2 mV *vs.* > −289 mV) (Hu et al., 2008), and as expected, more oxidizing in the ER relative to the cytosol, with the ER of Δ*glr1* slightly more oxidizing than Wt (−235 ± 3 mV *vs.* −242 ± 2 mV). Remarkably, $[GSx]_{ER}$ was in the close range, if not equal, to $[GSx]_{Cyt}$ as measured in both Δ*glr1* (31 ± 1 mM *vs* 31 ± 1 mM), and Wt (30 ± 2 mM *vs* 29.6 ± 2 mM), in contrast to $[GSSG]_{ER}$, which as measured in Δ*glr1* was more than twice its value in the cytosol (1.2 ± 0.03 mM *vs* 0.5 ± 0.03 mM).

## 2. A inhibitable facilitated diffusion of GSH across the ER membrane

Wt cells that overproduce the plasma membrane high-affinity GSH transporter Hgt1p, hereafter referred to as HGT1 cells, accumulate GSH to fairly high levels when supplied with GSH (Kumar et al., 2011). A $[GSx]_{Corr.Cyt}$ plateau of 250 mM is reached 1 h after medium addition of 60 μM GSH to the medium (Fig. 1A, Fig. S2A). We used HGT1 cells as a tool to monitor cytosol-to-ER fluxes of GSH, since this flux is amplified at high cellular GSH levels. To validate the $[GSx]_{TotCell}$ correction in these cells, we compared the HGT1-Δ*glr1* values of $[GSx]_{TotCell}$ and $[GSx]_{Cyt}$ 1 h after addition of increasing amounts of GSH. These values aligned together throughout the GSH titration, provided the 4.5-fold correction was applied to $[GSx]_{TotCell}$ (Fig. S2B). Incubating HGT1 cells 1 h with increasing GSH amounts led to an increase of $[GSx]_{ER}$ that tightly paralleled the $[GSx]_{Corr.Cyt}$ increase, up to a plateau lower than the $[GSx]_{Corr.Cyt}$ plateau (170 *vs.* 250 mM) reached at 30 μM GSH (Fig. 1A). Reduced GSH constituted most of the GSx that had entered the ER, thereby decreasing $E_{GSH.ER}$ (Fig. 1B, 1E). As glutaredoxins catalyze rxYFP equilibration with the GSH redox couple, we verified $E_{GSH.ER}$ using an ER-rxYFP-Grx1 fusion, which gave almost identical values (Fig. S2C). We also verified proper ER localization of the probes in HGT1 cells loaded with GSH by fluorescence microscopy, use of the rxYFP variant carrying a glycosylation site, and cell fractionation (Fig. S2D, S2E, S2F). Thus, $[GSx]_{Corr.Cyt}$ and $[GSx]_{ER}$ steady state values are in the same range (Table 1), and any increase in $[GSx]_{Corr.Cyt}$ causes a similar increase in $[GSx]_{ER}$, which suggests that GSH is imported

into the ER along its concentration gradient across the ER membrane. Importantly, the lower [GSx] plateau reached in the ER, relative to the cytosol, indicates that transport is inhibited when $[GSx]_{Corr.Cyt}$ ~170 mM. ER ingress of GSH activates Ero1 by reduction (Fig. S6) (Kumar et al., 2011). This was manifested here by a $[GSSG]_{ER}$ increase from 0.6 mM to a 4-mM plateau coincident with the $[GSx]_{ER}$ plateau, which slightly decreased $[GSH]_{ER}$/$[GSSG]_{ER}$ (Fig. 1C, 1D, S2G, S2H). Increased ER GSH levels caused ER stress, as shown by UPR-dependent *KAR2* induction (Kumar et al., 2011). The induction amplitude was also proportional to the amount of GSH added, up to a plateau reached at the levels of added GSH that inhibit GSH ER import (Fig. 1F).

The time-course of the HGT1 cells response to 30 μM GSH showed that $[GSx]_{Corr.Cyt}$ peaked at 170 mM, 1.5 h after GSH addition, and slowly declined to the pretreatment level at 7 h (Fig. 2A). Here again, $[GSx]_{ER}$ tightly paralleled the $[GSx]_{Corr.Cyt}$ increase, but interestingly, its decline was delayed, with $[GSx]_{ER}$ significantly higher than $[GSx]_{Corr.Cyt}$ at the 3 and 5 h time points (Fig. 2A, black arrow). This result suggests that the concentration-dependent transport that drives GSH ER ingress does not operate in reverse under this condition. Here again, reduced GSH constituted most of the GSx that entered the ER, along with Ero1-dependent $[GSSG]_{ER}$ increase, which interestingly was followed by an increase in $[GSSG]_{TotCell}$ (Fig. 2B, 2C). As the latter originates from Ero1 activity (Fig S2G, S2H), GSH must exit the ER, at least in part, upon conversion into GSSG. These perturbations in GSH and GSSG levels led to a transient decrease in both $E_{GSH}$ and the GSH/GSSG ratio in the ER (Fig. 2D, 2E). At 50 μM added GSH, $[GSx]_{Corr.Cyt}$ reached much higher values, relative to $[GSx]_{ER}$ (Fig. 2F), indicating again GSH transport inhibition (see Fig. 1A).

We conclude that GSH is transported from the cytosol to the ER along a concentration gradient, which suggests a facilitated diffusion, and hence the presence of a GSH transporter. Further, transport is inhibited when $[GSH]_{Cyt}$ reaches ~ 170 mM. Once the ER is saturated with GSH, GSH re-export to the cytosol appears inhibited.

### 3. A screen for a ER GSH transporter identifies Sec61

GSH becomes toxic at the high levels it reaches in HGT1 cells, inhibiting growth and causing cell death (Fig. S3A, S3B). This occurs mainly, if not exclusively, by impacting the ER since HGT1 cells lacking the UPR regulator Ire1p are sensitive to GSH at concentrations that are non-toxic to HGT1 cells (Kumar et al., 2011). Based on this notion, we assumed that impairment of the ER import of GSH should mitigate GSH toxicity, providing a means of screening for candidate GSH transporters. We screened null and temperature sensitive (*ts*) mutations of genes encoding ER transmembrane proteins that would both confer tolerance to HGT1-dependent GSH toxicity, without impairing GSH accumulation. We thereby identified the *sec61-2 ts* allele of the essential gene *SEC61*, which encodes the universally conserved ER protein-conducting channel (Deshaies and Schekman, 1987). In HGT1-*sec61-2* cells, GSH accumulation upon GSH addition was similar at the non-restrictive (24 °C) and restrictive (37 °C) temperatures, which indicated the correct plasma membrane expression of Hgt1p (Fig. 3A). In striking contrast, HGT1-*sec61-2* cells remained viable at 37 °C, whereas they lost viability at 24 °C, similar to HGT1 cells at both 24 °C and 37 °C (Fig. 3B). We sought to evaluate whether the increased resistance to GSH toxicity was due to defective ER

import of GSH by monitoring GSH cytosol-to-ER traffic via measurement of $E_{GSH.ER}$. However, ER-rxYFP was highly reduced at steady state in *sec61-2* cells due to probe mislocalization in the cytosol (Fig. S3C), thereby precluding this experiment.

In yeast, protein translocation into the ER occurs through either a cotranslational, signal recognition particle (SRP)-dependent pathway that uses the heterotrimeric Sec61 complex made of Sec61, Sbh1 and Sss1, or a post-translational translocation pathway that uses the heptameric Sec complex made of the Sec61 complex plus the Sec62–Sec63 complex (Mandon et al., 2013). SRP-dependent translocation also uses a Sec61-alternate translocon made of the Sec61-distantly related pore Ssh1, which complexes with Sbh2 and Sss1. Based on the above data, we reexamined the *sec62-1* (Deshaies and Schekman, 1990) and *sec63-1* (Rothblatt et al., 1989) *ts* mutants of the essential genes *SEC62* and *SEC63*. However, both mutants retained full HGT1-dependent GSH sensitivity at both 24 °C and 37 °C (Fig. 3C, 3D, and Fig. S3E, S3F).

These data suggest that the SRP-dependent, but not the post-translational protein translocation pathway, is involved in the ER import of GSH. We next sought further proof of the role of Sec61 in this transport.

## 4. Both Sec61 and Ssh1 transport GSH into the ER

The ten transmembrane (TM) spans of Sec61 are arranged into two halves that form an hourglass-shaped pore with a middle ring and a lateral gate between transmembrane domain 2 (TM2) and TM7 facing the lipid phase. Its lumenal face is filled by the plug domain, a reentry loop preceding TM2 (Park and Rapoport, 2012). In the Sec61 closed conformation, the lateral gate is closed, and both the ring and plug domain maintain the channel permeability seal. In yeast, a gating motif that links the Sec61 lateral gate and plug domain regulates the transition from the closed to open channel conformation (Trueman et al., 2012). The *sec61ΔL7* mutant lacks the entire lumenal loop 7 adjacent to the lateral gate motif, which impairs transition from the closed to the open conformation, thereby causing defective post-translational translocation, slow growth and cold sensitivity (Tretter et al., 2013). When transformed with HGT1, the *sec61ΔL7* mutant accumulated GSH as Wt, which indicated correct Hgt1p plasma membrane expression, but was highly resistant to GSH-induced cell death (Fig. 4A, 4B, S4B). Furthermore, in HGT1-*sec61ΔL7*, the decrease of $E_{GSH.ER}$ observed in HGT1 cells on addition of 30 μM GSH was severely blunted if not absent (Fig. 4C), thus indicating defective ER import of GSH, in agreement with the viability assay. The N302 residue in TM7 is part of the Sec61 gating motif (Trueman et al., 2012); its substitution to a hydrophobic (N302L) or polar residue (N302D) stabilizes Sec61 in the closed or open conformation, respectively. Consistent with the previous result, in the $sec61^{N302L}$ mutant the decrease of $E_{GSH.ER}$ on addition of 30 μM GSH was also dampened, thus confirming that mutations stabilizing the Sec61 closed conformation prevent the ER import of GSH (Fig. 4D). Strikingly, expression of $sec61^{N302L}$ in a strain lacking *SSH1* (Δ*ssh1*) further impaired transport (Fig. 4D), thus suggesting a redundancy of Sec61 and Ssh1 in GSH transport. In contrast, the $Sec61^{N302D}$ mutation, which stabilizes the open conformation, did not alter the ER import of GSH (Fig. 4E). HGT1-dependent cellular GSH accumulation (Fig. S4C) and proper ER localization of ER-rxYFP (Fig. S3C, S3D) was

verified for these and the others *sec61* mutants and conditions tested here. In yeast, entire removal of the Sec61 plug domain (Δplug) causes a *prl* phenotype, i.e. the suppression of signal sequence mutations, but no growth defects at any temperature (Junne et al., 2006). In contrast to the above Sec61 mutations, the ER transport of GSH in the Δplug mutant was similar to Wt on addition of 30 μM GSH (Fig. 4F), but differed from the latter at 50 μM (Fig. 4G). At this higher GSH, ER reduction was further increased, indicating loss of transport inhibition.

To further establish the role of Sec61 in GSH transport, we sought to identify conditions under which it becomes operative. Puromycin (Pm), which causes premature chain termination, empties ER translocon pores by release of the nascent chain into the ER lumen without ribosome-pore detachment (Simon and Blobel, 1991). We overproduced Hgt1p in a strain made Pm-sensitive by inactivation of the pleiotropic-drug resistance transcription factors Pdr1 and Pdr3 and the methyltransferase Erg6 (Δ*erg6*Δ*pdr1*Δ*pdr3*) (Cary et al., 2014). In this strain, a 15-min treatment with 2 mM Pm did not prevent, but at slightly increased reduction of the ER with addition of 50 μM GSH relative to Pm-untreated cells (Fig. 4H), which indicates that the ER import of GSH does not require *de novo* protein synthesis. Cycloheximide (CHX) traps the nascent chain within the channel by blocking the translocation step in translation elongation and stabilizes ribosomes on the ER membrane (Schneider-Poetsch et al., 2010). Strikingly, a 10-min treatment with CHX totally prevented reduction of the ER (Fig. 4I), despite normal cellular GSH accumulation (Fig S4E). Hence, actively translating ribosomes bound to translocons effectively prevent GSH transport. The almost total inhibitory effect of CHX may also indicate that it increases the density of active ER membrane ribosome-bound pores by decreasing their turnover. We next tested whether idle ribosome binding to translocons is required for GSH transport. Sec61 mutations impairing ribosome binding did not allow proper co-expression of HGT1 and ER-rxYFP. We instead used a plasmid-borne galactose-inducible dominant allele of *SRP54* (*SRP54*$^{dn}$) defective in GTP hydrolysis, which locks and inactivates the SRP receptor (Mutka and Walter, 2001). We found that 3 h after Gal1-SRP54$^{dn}$ induction in HGT1 cells, reduction of the ER upon GSH incubation was decreased relative to cells carrying Gal-SRP54 (Fig. 4J), despite normal HGT1-dependent GSH accumulation (Fig. S4D). Longer inhibition of the SRP pathway was not tested since this impaired HGT1 and ER-rxYFP expression. By sequestering the SRP receptor into an inactive pool (Mutka and Walter, 2001), SRP54$^{dn}$ should decrease the ER content of both active and inactive ribosome-bound translocons. However, since the effect of CHX excludes the former, the effect of SRP54$^{dn}$, even partial, is suggestive of a requirement for inactive ribosome-bound translocons.

Collectively, these data indicate that the Sec61 and Ssh1 translocons serve to transport GSH across the ER membrane, and suggest that this transport requires the presence of inactive ribosomes bound to translocons. Furthermore, whereas the Sec61 closed conformation prevents GSH transport, the plug domain contributes to the mechanism of transport inhibition.

### 5. Oxidized Kar2 inhibits the ER import of GSH

The ER chaperone Kar2 (Bip) is oxidized to a sulfenic acid at residue Cys63 in cells overexpressing Ero1$^{C150–C295}$, a mutant that is constitutively active due to the lack of negative regulatory disulfides (see introduction). In turn, Kar2 mutants mimicking its oxidized form mitigate Ero1$^{C150–C295}$ toxicity (Wang et al., 2014). Given Sec61's role in GSH transport, Kar2's contribution to Sec61 protein translocation (Mandon et al., 2013), and GSH activation of Ero1 (Fig. S6) (Kumar et al., 2011), we examined the involvement of Kar2 in GSH transport. We probed Kar2 oxidation by differential labeling of reduced *vs.* oxidized Cys residues with NEM and PEG-maleimide, respectively, which upshifts oxidized Kar2 SDS-PAGE migration (Fig. 5A, Fig. S5A, S5B). A 2-h incubation with GSH triggered Kar2 oxidation, the degree of which was proportional to the amount of added GSH, up to a maximum at 20–30 μM (Fig. 5B). A time-course response to 50 μM GSH showed that oxidation was maximal between 1–4 h and remained so longer than 6 h (Fig. 5C, Fig. S6). To test whether Kar2 oxidation alters GSH toxicity, we used mutants with substitution of Cys63 to either Ala (Kar2$^{C63A}$) or Trp (Kar2$^{C63W}$), which mimic the reduced and sulfenylated forms of Kar2, respectively (Wang et al., 2014). *kar2-C63A* is fully viable, whereas *KAR2-C63W* is unviable and must be complemented by *KAR2* (Wang et al., 2014). We found that, relative to HGT1 cells, HGT1-*kar2-C63A* was more sensitive to GSH by both growth plate and survival assays, whereas HGT1-*kar2-C63W* was much more resistant (Fig. 5D, 5E, 5F), despite normal HGT1-dependent GSH accumulation (Fig. S4F). Consistent with the sensitivity assays, the ER import of GSH in HGT1-*kar2-C63A* was not only fully maintained, but as seen with the Δplug mutant, not anymore inhibited, with $[GSx]_{ER}$ equilibrating with $[GSx]_{Corr.Cyt}$ at the very high peak value of 250 mM, 2 h after addition of 50 μM GSH (Fig. 5G, 5H). In contrast, ER import of GSH was severely blunted in HGT1 cells expressing *Kar2-C63W*, with $[GSx]_{ER}$ never above 45 mM relative to the high $[GSx]_{Corr.Cyt}$ values of 120 and 230 mM seen at 30 and 50 μM added GSH, respectively (Fig. 5G, 5H).

Kar2 is presumably oxidized by the $H_2O_2$ side product of Ero1 catalysis (Tu and Weissman, 2002). We thus sought to probe the causal link between Kar2 oxidation, Ero1 reductive activation and GSH transport inhibition, using the *ero1-1 ts* mutant (Frand and Kaiser, 1999) to blunt the ER source of $H_2O_2$. Unexpectedly however, Kar2 was oxidized in HGT1-*ero1-1* cells at the non-restrictive temperature (24 °C) prior to GSH addition (Fig. 5I). Oxidation increased at 37 °C, possibly by ROS originating from mitochondria, but not after GSH addition (Fig. 5I). We took advantage of Kar2 constitutive oxidation in *ero1-1* to directly probe the effect of this modification on GSH transport. At 37 °C, the ER was too reducing to allow any measurements in the HGT1-*ero1-1* strain due to lack of Ero1 activity. However, we found that at 30 °C, GSH transport was substantially inhibited (Fig. 5J), confirming the link between Kar2 oxidation and GSH transport inhibition. We also found that Kar2 was not oxidized in Δ*ire1* with GSH addition (Fig. 5K), as a result of Ero1 defective UPR induction (see below), which increased the threshold GSH transport inhibition relative to Wt (Fig. 5L, M, Fig. S4G, S4H).

These data indicate that oxidation of Kar2 provides the molecular basis for the inhibitable nature of GSH transport into the ER, also corroborating the role of Sec61 in this transport.

### 6. A tight coupling between UPR-dependent Ero1 induction and ER import of GSH

As suggested above, by triggering Ero1-dependent Kar2 oxidation, GSH regulates its own import into the ER. To further establish the coupling between ER GSH import, Ero1 activity and Kar2 oxidation, we monitored the GSH dependence of Kar2 oxidation by Ero1, using the Δ*gsh1* strain that cannot synthesize GSH. In Wt cells, $Ero1^{C150AC295A}$ (Wang et al., 2014) or Ero1 overproduction from a galactose-inducible promoter both triggered Kar2 oxidation (Fig. 6A). In Δ*gsh1* however, although Kar2 became oxidized, oxidation was now transient (Fig. 6A), disappearing with the degree of GSH depletion (Fig. 6B), thus confirming the link between ER import of GSH, Ero1 activation, and Kar2 oxidation. We reciprocally tested the influence of $Ero1^{C150AC295A}$ overproduction on the ER import of GSH, in which facilitated diffusion of GSH is expected to be stimulated by Ero1-dependent conversion of GSH into GSSG. When $Ero1^{C150AC295A}$ was induced, $[GSx]_{ER}$ indeed steadily increased up to 80 mM at 8 h, but unexpectedly $[GSx]_{Corr.Cyt}$ also increased to a similar value (Fig. 6C, 6D). Simultaneous increase in both Ero1 activity and $[GSx]_{Corr.Cyt}$ masked which of the two triggers ER import of GSH. Since perturbation is initiated in the ER, the latter should be a consequence of the former, at least initially, and hence that coupling between GSH import and Ero1 activity is reciprocal. Overproducing Wt Ero1 similarly increased both $[GSx]_{ER}$ and $[GSx]_{Corr.Cyt}$, albeit to lower levels (Fig. 6C, 6D).

To determine whether the defective Kar2 oxidation in Δ*ire1* (see Fig. 5K) is due to faulty Ero1 induction by a disabled UPR, we overproduced Ero1 or its hyperactive mutant in Δ*ire1*. This indeed restored Kar2 oxidation (Fig. 6A, lower panel), thus indicating that UPR-induced *de novo* Ero1 synthesis is critical in the coupling between Ero1 and GSH transport.

We lastly explored the Ero1-GSH interplay, this time under ER stress caused by tunicamycin (Tm). In Wt, addition of 1 μg Tm led to an increase of $[GSx]_{ER}$ from 30 up to 60 mM at 2 h, which as in cells overexpressing Ero1, was accompanied by a similar increase of $[GSx]_{Corr.Cyt}$ (Fig. 6H). Tm at 0.25 and 0.1 μg also triggered $[GSx]_{ER}$ and $[GSx]_{Corr.Cyt}$ increases of amplitude proportional to the amount of Tm (Fig. 6F, 6G). In keeping with the ER import of GSH, Tm also led to Ero1 activation, as indicated by Kar2 oxidation, with the higher dose of the stressor generating a faster oxidation response (Fig. 6I).

In conclusion, our data establish a reciprocal interplay between ER import of GSH and activation of Ero1, which appears integral to the UPR during ER stress (Fig. 6J).

## Discussion

As we showed here, GSH is transported into the ER in *S. cerevisiae* by facilitated diffusion through the universally conserved ER protein-conducting channel Sec61, with oxidized Kar2 inhibiting this transport. Upon import into the ER, GSH in turn inhibits its import by triggering $H_2O_2$-dependent Kar2 (Bip) oxidation through Ero1 reductive activation, which indicates reciprocal control between ER GSH import and Ero1 activation (Fig. 6J). We also demonstrated that ER stress stimulates the regulated transport of GSH by increasing the levels of both cellular GSH and Ero1. Such reciprocal control of the opposing ER thiol-oxidizing and reducing pathways appears essential for subtle homeostatic control of ER redox poise. This control prevents excessive Ero1 activity which underlies the toxicity of

both overproduction of hyperactive Ero1 (Wang et al., 2014) and high cellular GSH levels (Kumar et al., 2011). This reciprocal regulation might also be important to satisfy the requirements for oxidative protein folding during ER stress by simultaneously promoting a transient increase in Ero1-dependent thiol oxidation and extra GSH reducing power. These data also suggest that the ER membrane is permeable to other small molecules in addition to GSH.

## Reciprocal control of Ero1 activity and ER import of GSH

The ER transport mechanism of GSH into the ER includes four critical features. **(i)** The facilitated diffusion of reduced GSH that follows the concentration gradient across the ER membrane is essential for maintaining ER GSH homeostasis, as it compensates for the GSH consumed in the ER by Ero1-dependent oxidation. Such facilitated GSH diffusion has been suggested in mammals based on an *in vitro* microsome transport assay (Banhegyi et al., 1999). **(ii)** The transport of GSH is inhibited by the oxidized form of Kar2. These two features establish a reciprocal regulation between GSH import and activation of Ero1, since Kar2 oxidation is a function of Ero1 activity and Ero1 is activated by (indirect) reduction by GSH (see Fig. 6J). The two other features are seen during ER stress, which activate the transport mechanism. **(iii)** The unexpected increase in cytosolic GSH levels during ER stress, the levels of which are commensurate to stress intensity (see Fig. 6C–H), yields a net import of reducing equivalents in the ER. **(iv)** The level of Ero1 set by the UPR, in turn sets both the rate of GSH consumption and the levels of $H_2O_2$ produced. The critical role of the latter in the regulation of GSH transport is reflected by lack of Kar2 oxidation and hence of GSH transport inhibition in cells with a disabled UPR (see Fig. 5K, 5L, 5M). Hence, ER stress stimulates GSH transport in a manner proportional to its intensity, by setting the magnitude of both $[GSH]_{Cyt}$ increase and UPR-dependent Ero1 induction. This effect is reflected by the observation that the concerted increase in $[GSH]_{Cyt}$ and $[GSH]_{ER}$ and speed of Kar2 oxidation are proportionate to the amount of tunicamycin used (see Fig. 6F–I). We thus surmise that activation of GSH transport under ER stress is an amplification of the process occurring during non-stress conditions.

This model was established in the HGT1 cell model, due to its unique ability to very rapidly accumulate GSH to fairly high levels. However, the $[GSH]_{ER}$ levels reached in HGT1 cells were much higher than those reached both on Tm exposure and upon hyperactive Ero1 overproduction. We suggest that the high $[GSH]_{ER}$ levels reached in HGT1 cells are the consequence of the rapidity of their buildup, occurring prior to the regulation of GSH transport via the UPR-dependent activation of Ero1 that induces the Kar2-dependent negative regulatory loop.

## Glutathione as the main ER reducing power

Efficiency of denatured protein refolding by PDI *in vitro* is not a function of disulfide formation, but rather disulfide isomerization for which reduced glutathione has a crucial role (Lyles and Gilbert, 1991). While several studies suggest that GSH provides the reducing power for ER oxidative folding and for buffering Ero1 oxidizing activity (Chakravarthi and Bulleid, 2004; Cuozzo and Kaiser, 1999; Molteni et al., 2004), the observation that oxidative folding remains intact upon purging the mammalian ER of GSH has suggested that it is

dispensable in the ER (Tsunoda et al., 2014). However, the importance of GSH to ER redox control is supported by the observation that GSH becomes a potent ER reducing power when at high levels (Kumar et al., 2011), and the current data indicating a net ER import of GSH at least under Tm-induced ER stress, followed by Ero1 reductive activation. The twofold concerted increase in $[GSH]_{Cyt}$ and $[GSH]_{ER}$ and corresponding $E_{GSH}$ decrease from −240 to −257 mV on Tm exposure, together with the consequential Ero1 activation, is a probable adaptive measure to ER stress protein misfolding. ER stress also stimulates GSH biosynthesis in *A. thaliana* (Ozgur et al., 2015), and in mammals by PERK-dependent Atf4 induction (Harding et al., 2003). Furthermore, ER stress caused by Tm in Atf4-deficient *C. elegans* (Harding et al., 2003) and by coagulation factor VIII expression in mouse hepatocytes (Malhotra et al., 2008) is associated with a 50% decrease of total GSH. In *C. elegans*, this decrease is rescued by inactivating Ero1, which highlights the conservation of the functional interplay between GSH and Ero1 established here, and the importance of GSH for ER redox metabolism.

## ER transport of GSH by idle ribosome-bound translocons

Our data provide compelling evidence that both Sec61 and Ssh1 serve as GSH conduits to the ER, while ruling out a role of the Sec complex (Fig. 3, 4, Fig S3). The presence of both gain and loss of function associated with Sec61 genetic modifications, and the absence of effect of the translation inhibitor puromycin, rule out an indirect effect. Inhibition of GSH transport by oxidized Kar2, which contributes to the Sec61 polypeptide translocation mechanism (Mandon et al., 2013), further supports this conclusion. The aggravation of the $Sec61^{N302L}$ GSH transport defect by deletion of *SSH1* (see Fig. 4D), indicates that both Sec61 and Ssh1 transport GSH. The existence of another transporter cannot be ruled out, but it would have a minor function, given the major GSH phenotypes of the *SEC61* mutants. Translocons are present in the ER membrane as unbound, or bound by inactive or active ribosomes (Reid and Nicchitta, 2015). Those bound by active ribosomes do not allow GSH transport, as indicated by total transport inhibition by CHX, which by blocking the translocation step in translation elongation, traps the nascent chain within the channel (Schneider-Poetsch et al., 2010). Of the two remaining states of Sec61, the ones bound by idle ribosomes are those that appear permissive to GSH transport, as suggested by partial transport inhibition upon $Srp54^{dn}$ overproduction (see Fig. 4J). By sequestering the SRP receptor into an inactive pool (Mutka and Walter, 2001), this mutant should decrease the ER content of both active and inactive ribosome-bound translocons, but the former are excluded by the effect of CHX. This conclusion is consistent with *in vitro* electrophysiological data that indicate that ER membrane permeability to ions and small molecules is due to idle ribosome-bound pores in both mammals and prokaryotes (Heritage and Wonderlin, 2001; Knyazev et al., 2013; Lizak et al., 2006; Simon and Blobel, 1991). It is also compatible with the structural changes of the channel triggered by idle ribosome binding, which consist of a partial opening of the lateral gate together with destabilization of the interaction between the plug and pore ring (Pfeffer et al., 2015; Zimmer et al., 2008). Disruption of plug-ring interactions might thus suffice to allow GSH-facilitated diffusion.

Channel gating of GSH by idle ribosomes raises the question of their availability. In semi-permeabilized mammalian cells, puromycin increases Sec61-dependent transport of a small

molecule above a basal level, which indicates recruitment of additional pores (Heritage and Wonderlin, 2001). In contrast, the ER transport of GSH is insensitive to puromycin, which suggests the presence of an invariant number of idle ribosome-bound translocons dedicated to GSH transport.

### Translocon gating by oxidized Kar2 regulates the ER transport of GSH

Mutation in the lateral gate motif ($Sec61^{N302L}$) (Trueman et al., 2012) and deletion of loop 7 (Sec61ΔL7) (Tretter et al., 2013), which both stabilize the closed channel conformation, almost totally inhibited GSH transport (see Fig. 4C, 4D). This observation could indicate that transport is allowed only when the channel is in the open conformation. However, the N302D mutation that stabilizes the open conformation (Trueman et al., 2012) did not impact transport (see Fig. 4E), whereas deletion of the plug domain (Δplug), which also stabilizes the channel open conformation (Junne et al., 2006; Trueman et al., 2012), resulted in the loss of GSH transport inhibition (see Fig. 4F, 4G), as also seen with $Kar2^{C63A}$ and oxidized Kar2 (see Fig. 5G–J). The latter data thus rather suggest that the plug is the critical Sec61 structural feature in GSH gating. In mammals, binding of the Kar2 mammalian homologue Bip to loop 7 prevents Sec61-dependent ER leakage of calcium, presumably by inducing pore closure (Schauble et al., 2012). From this result, we infer that oxidized Kar2 in yeast binds to loop 7, thereby reversing the idle ribosome-induced partial open conformation, and in particular restoring the plug-ring interactions (see above). The much higher values of $[GSx]_{ER}$ relative to $[GSx]_{Corr.Cyt}$ during the declining phase of the GSH response indicated that facilitated diffusion governing the ER import of GSH did not operate in reverse (see Fig. 2A). This result might be explained by either channel closure by oxidized Kar2 or direction of plug domain displacement within the pore lumenal face only allowing a cytosol-to-ER flux. However, the Sec61-dependent ER leakage of calcium upon Bip depletion (Schauble et al., 2012) supports the former hypothesis.

Two distinct models have been proposed regarding regulation of the channel permeability barrier in the ER. In prokaryotes, the plug domain is suggested to play a critical role (Park and Rapoport, 2012), while in eukaryotes, Bip/Kar2 fulfills this function (Hamman et al., 1998). Our data reconcile these two models by showing that the ER protein channel is in fact permeable, but that this permeability is not constitutive but regulated in yeast by both oxidized Bip and the plug domain. From the ER transport of GSH demonstrated here, we suggest that the ER membrane is permissive to the facilitated diffusion of any small molecules of size at least equivalent to GSH.

## Methods

### Strains, plasmids and growth conditions

Strains and plasmids are listed in Supplemental Tables S1 and S2. See supplemental experimental procedures.

### Glutathione enzymatic measurement

Total GSH was measured using the DTNB colorimetric assay as described in the supplemental experimental procedures.

### Redox western blots

The *in vivo* redox state of rxYFP, 1-Cys-Grx1 and Kar2 were determined by redox western blots. See supplemental experimental procedures.

### Calculation of redox potentials and GSH absolute subcellular concentration

The rxYFP redox ratio determined by redox western was used to calculate $E_{GSH}$ by the Nernst equation. The 1-Cys-Grx1 redox ratio determined by redox western was used to calculate the GSH/GSSG ratio using $K_{ox} = 74 \pm 6$ (Iversen et al., 2010). GSH absolute concentration was calculated using $[GSH]^2/[GSSG]$ derived from $E_{GSH}$ and GSH/GSSG as described (Montero et al., 2013). See supplemental experimental procedures for details.

## Supplementary Material

Refer to Web version on PubMed Central for supplementary material.

## Acknowledgments

We are indebted to C. Sevier, R. Gilmore, K. Romisch, P. Walter, and M. Spiess for their generous gifts of strains and plasmids. Thanks to R. Sitia for his comments on the manuscript. This work was funded by grants from ANR (ERRed) and InCA (PLBIO INCA_5869) to MBT, NIH (GM086619 and GM118164) to CEO. AP was supported by a CEA IRTELIS PhD fellowship.

## References

Banhegyi G, Lusini L, Puskas F, Rossi R, Fulceri R, Braun L, Mile V, di Simplicio P, Mandl J, Benedetti A. Preferential transport of glutathione versus glutathione disulfide in rat liver microsomal vesicles. J Biol Chem. 1999; 274:12213–12216. [PubMed: 10212186]

Cary GA, Yoon SH, Torres CG, Wang K, Hays M, Ludlow C, Goodlett DR, Dudley AM. Identification and characterization of a drug-sensitive strain enables puromycin-based translational assays in Saccharomyces cerevisiae. Yeast. 2014; 31:167–178. [PubMed: 24610064]

Chakravarthi S, Bulleid NJ. Glutathione is required to regulate the formation of native disulfide bonds within proteins entering the secretory pathway. J Biol Chem. 2004; 279:39872–39879. [PubMed: 15254031]

Cuozzo JW, Kaiser CA. Competition between glutathione and protein thiols for disulphide-bond formation. Nat Cell Biol. 1999; 1:130–135. [PubMed: 10559898]

Delic M, Mattanovich D, Gasser B. Monitoring intracellular redox conditions in the endoplasmic reticulum of living yeasts. FEMS Microbiol Lett. 2010; 306:61–66. [PubMed: 20337710]

Deshaies RJ, Schekman R. A yeast mutant defective at an early stage in import of secretory protein precursors into the endoplasmic reticulum. J Cell Biol. 1987; 105:633–645. [PubMed: 3305520]

Deshaies RJ, Schekman R. Structural and functional dissection of Sec62p, a membrane-bound component of the yeast endoplasmic reticulum protein import machinery. Mol Cell Biol. 1990; 10:6024–6035. [PubMed: 2233730]

Frand AR, Kaiser CA. Ero1p oxidizes protein disulfide isomerase in a pathway for disulfide bond formation in the endoplasmic reticulum. Mol Cell. 1999; 4:469–477. [PubMed: 10549279]

Hamman BD, Hendershot LM, Johnson AE. BiP maintains the permeability barrier of the ER membrane by sealing the lumenal end of the translocon pore before and early in translocation. Cell. 1998; 92:747–758. [PubMed: 9529251]

Harding HP, Zhang Y, Zeng H, Novoa I, Lu PD, Calfon M, Sadri N, Yun C, Popko B, Paules R, et al. An integrated stress response regulates amino acid metabolism and resistance to oxidative stress. Mol Cell. 2003; 11:619–633. [PubMed: 12667446]

Heritage D, Wonderlin WF. Translocon pores in the endoplasmic reticulum are permeable to a neutral, polar molecule. J Biol Chem. 2001; 276:22655–22662. [PubMed: 11303028]

Hu J, Dong L, Outten CE. The redox environment in the mitochondrial intermembrane space is maintained separately from the cytosol and matrix. J Biol Chem. 2008; 283:29126–29134. [PubMed: 18708636]

Iversen R, Andersen PA, Jensen KS, Winther JR, Sigurskjold BW. Thiol-disulfide exchange between glutaredoxin and glutathione. Biochemistry. 2010; 49:810–820. [PubMed: 19968277]

Junne T, Schwede T, Goder V, Spiess M. The plug domain of yeast Sec61p is important for efficient protein translocation, but is not essential for cell viability. Mol Biol Cell. 2006; 17:4063–4068. [PubMed: 16822836]

Knyazev DG, Lents A, Krause E, Ollinger N, Siligan C, Papinski D, Winter L, Horner A, Pohl P. The bacterial translocon SecYEG opens upon ribosome binding. J Biol Chem. 2013; 288:17941–17946. [PubMed: 23645666]

Kumar C, Igbaria A, D'Autreaux B, Planson AG, Junot C, Godat E, Bachhawat AK, Delaunay-Moisan A, Toledano MB. Glutathione revisited: a vital function in iron metabolism and ancillary role in thiol-redox control. EMBO J. 2011; 30:2044–2056. [PubMed: 21478822]

Lizak B, Czegle I, Csala M, Benedetti A, Mandl J, Banhegyi G. Translocon pores in the endoplasmic reticulum are permeable to small anions. Am J Physiol Cell Physiol. 2006; 291:C511–517. [PubMed: 16611737]

Lyles MM, Gilbert HF. Catalysis of the oxidative folding of ribonuclease A by protein disulfide isomerase: dependence of the rate on the composition of the redox buffer. Biochemistry. 1991; 30:613–619. [PubMed: 1988050]

Malhotra JD, Miao H, Zhang K, Wolfson A, Pennathur S, Pipe SW, Kaufman RJ. Antioxidants reduce endoplasmic reticulum stress and improve protein secretion. Proc Natl Acad Sci U S A. 2008; 105:18525–18530. [PubMed: 19011102]

Mandon EC, Trueman SF, Gilmore R. Protein translocation across the rough endoplasmic reticulum. Cold Spring Harb Perspect Biol. 2013:5.

Margittai E, Sitia R. Oxidative protein folding in the secretory pathway and redox signaling across compartments and cells. Traffic. 2011; 12:1–8. [PubMed: 20716108]

Molteni SN, Fassio A, Ciriolo MR, Filomeni G, Pasqualetto E, Fagioli C, Sitia R. Glutathione limits Ero1-dependent oxidation in the endoplasmic reticulum. J Biol Chem. 2004; 279:32667–32673. [PubMed: 15161913]

Montero D, Tachibana C, Rahr Winther J, Appenzeller-Herzog C. Intracellular glutathione pools are heterogeneously concentrated. Redox Biol. 2013; 1:508–513. [PubMed: 24251119]

Morgan B, Ezerina D, Amoako TN, Riemer J, Seedorf M, Dick TP. Multiple glutathione disulfide removal pathways mediate cytosolic redox homeostasis. Nat Chem Biol. 2013; 9:119–125. [PubMed: 23242256]

Mutka SC, Walter P. Multifaceted physiological response allows yeast to adapt to the loss of the signal recognition particle-dependent protein-targeting pathway. Mol Biol Cell. 2001; 12:577–588. [PubMed: 11251072]

Ostergaard H, Tachibana C, Winther JR. Monitoring disulfide bond formation in the eukaryotic cytosol. J Cell Biol. 2004; 166:337–345. [PubMed: 15277542]

Ozgur R, Uzilday B, Sekmen AH, Turkan I. The effects of induced production of reactive oxygen species in organelles on endoplasmic reticulum stress and on the unfolded protein response in arabidopsis. Ann Bot. 2015; 116:541–553. [PubMed: 26070642]

Park E, Rapoport TA. Mechanisms of Sec61/SecY-mediated protein translocation across membranes. Annu Rev Biophys. 2012; 41:21–40. [PubMed: 22224601]

Pfeffer S, Burbaum L, Unverdorben P, Pech M, Chen Y, Zimmermann R, Beckmann R, Forster F. Structure of the native Sec61 protein-conducting channel. Nat Commun. 2015; 6:8403. [PubMed: 26411746]

Pollard MG, Travers KJ, Weissman JS. Ero1p: a novel and ubiquitous protein with an essential role in oxidative protein folding in the endoplasmic reticulum. Mol Cell. 1998; 1:171–182. [PubMed: 9659914]

Reid DW, Nicchitta CV. Diversity and selectivity in mRNA translation on the endoplasmic reticulum. Nat Rev Mol Cell Biol. 2015; 16:221–231. [PubMed: 25735911]

Rothblatt JA, Deshaies RJ, Sanders SL, Daum G, Schekman R. Multiple genes are required for proper insertion of secretory proteins into the endoplasmic reticulum in yeast. J Cell Biol. 1989; 109:2641–2652. [PubMed: 2687285]

Schauble N, Lang S, Jung M, Cappel S, Schorr S, Ulucan O, Linxweiler J, Dudek J, Blum R, Helms V, et al. BiP-mediated closing of the Sec61 channel limits Ca2+ leakage from the ER. EMBO J. 2012; 31:3282–3296. [PubMed: 22796945]

Schneider-Poetsch T, Ju J, Eyler DE, Dang Y, Bhat S, Merrick WC, Green R, Shen B, Liu JO. Inhibition of eukaryotic translation elongation by cycloheximide and lactimidomycin. Nat Chem Biol. 2010; 6:209–217. [PubMed: 20118940]

Sevier CS, Qu H, Heldman N, Gross E, Fass D, Kaiser CA. Modulation of cellular disulfide-bond formation and the ER redox environment by feedback regulation of Ero1. Cell. 2007; 129:333–344. [PubMed: 17448992]

Simon SM, Blobel G. A protein-conducting channel in the endoplasmic reticulum. Cell. 1991; 65:371–380. [PubMed: 1902142]

Toledano MB, Kumar C, Le Moan N, Spector D, Tacnet F. The system biology of thiol redox system in Escherichia coli and yeast: differential functions in oxidative stress, iron metabolism and DNA synthesis. FEBS Lett. 2007; 581:3598–3607. [PubMed: 17659286]

Tretter T, Pereira FP, Ulucan O, Helms V, Allan S, Kalies KU, Romisch K. ERAD and protein import defects in a sec61 mutant lacking ER-lumenal loop 7. BMC Cell Biol. 2013; 14:56. [PubMed: 24314051]

Trueman SF, Mandon EC, Gilmore R. A gating motif in the translocation channel sets the hydrophobicity threshold for signal sequence function. J Cell Biol. 2012; 199:907–918. [PubMed: 23229898]

Tsunoda S, Avezov E, Zyryanova A, Konno T, Mendes-Silva L, Pinho Melo E, Harding HP, Ron D. Intact protein folding in the glutathione-depleted endoplasmic reticulum implicates alternative protein thiol reductants. Elife. 2014; 3:e03421. [PubMed: 25073928]

Tu BP, Weissman JS. The FAD- and O(2)-dependent reaction cycle of Ero1-mediated oxidative protein folding in the endoplasmic reticulum. Mol Cell. 2002; 10:983–994. [PubMed: 12453408]

Wang J, Pareja KA, Kaiser CA, Sevier CS. Redox signaling via the molecular chaperone BiP protects cells against endoplasmic reticulum-derived oxidative stress. Elife. 2014; 3:e03496. [PubMed: 25053742]

Zimmer J, Nam Y, Rapoport TA. Structure of a complex of the ATPase SecA and the protein-translocation channel. Nature. 2008; 455:936–943. [PubMed: 18923516]

## Highlights

- Transport of glutathione (GSH) into the ER proceeds via facilitated diffusion
- The protein-conducting channel Sec61 transports GSH into the ER
- Oxidized Bip (Kar2) inhibits entry of GSH into the ER
- GSH import into the ER and Ero1 activation are reciprocally regulated

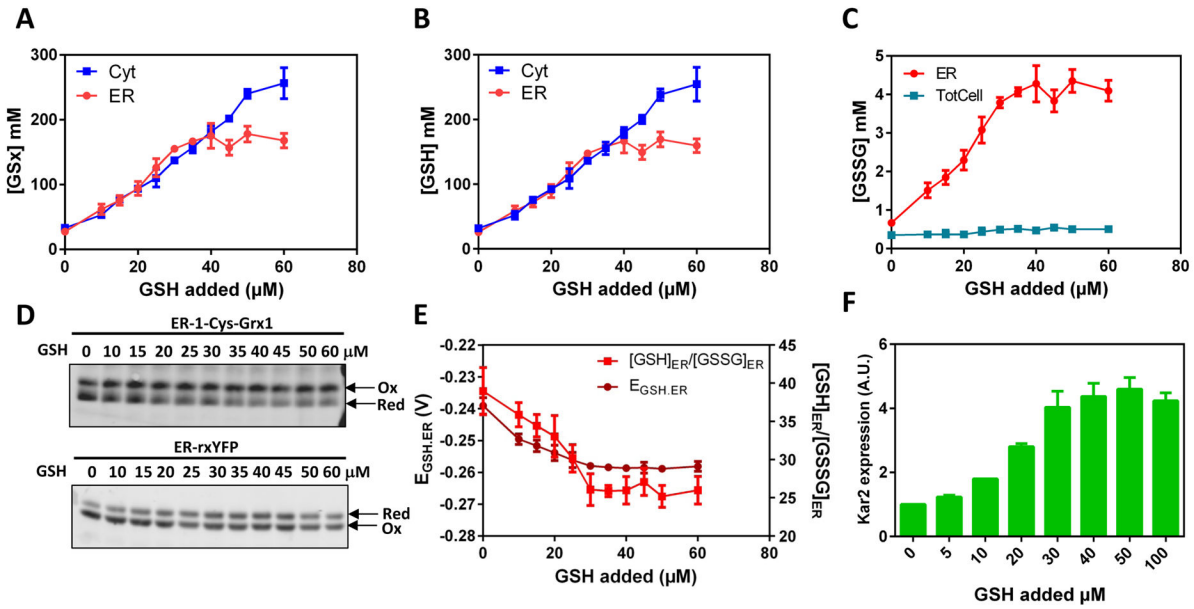


**Figure 1. Inhibitable facilitated diffusion of GSH across the ER membrane**

Corrected cytosolic (Cyt) (TotCell x 4.5), total cellular (TotCell) and ER (ER) levels of **(A)** [GSx] = [GSH] + 2[GSSG], **(B)** reduced [GSH] and **(C)** oxidized [GSSG] in mM, as indicated, measured in HGT1 cells incubated 1 h with the indicated amount of GSH. **(D)** Non-reducing SDS-PAGE migration of ER-1-Cys-Grx1 (upper panel) and ER-rxYFP (lower panel) from lysates of HGT1 cells incubated with indicated amount of GSH for 1h, representative of those used to derive the data in E. **(E)** The ER glutathione redox potential ($E_{GSH.ER}$), and ER ratio of GSH/GSSG values used to derive the data in A–C. **(F)** *KAR2* expression measured by quantitative PCR in HGT1 cells incubated 1 h with the indicated amount of GSH. Values are the mean of three independent biological replicas ± standard deviation (s.d.).

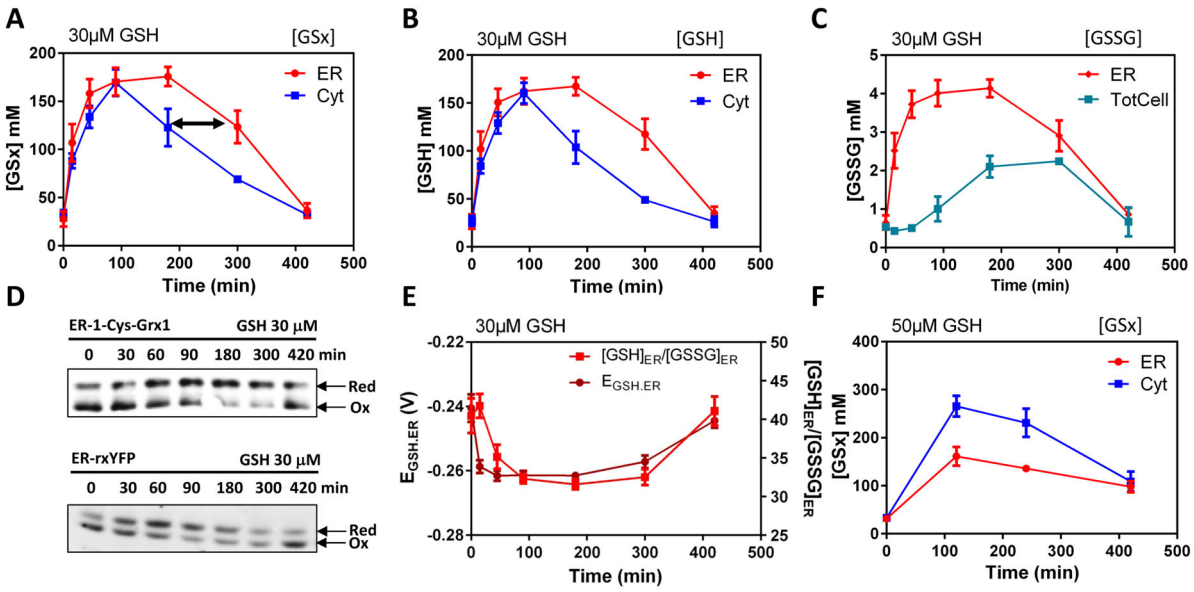


**Figure 2. The time-dependent facilitated diffusion of glutathione in the ER at high GSH cytosolic concentrations**

Corrected cytosolic (Cyt), total cellular (TotCell) and ER (ER) levels, as indicated, of **(A)** [GSx] = [GSH] + 2[GSSG], **(B)** reduced [GSH] and **(C)** oxidized [GSSG] measured in HGT1 cells incubated with 30 μM GSH for the indicated time. **(D)** Non-reducing SDS-PAGE migration of ER-1-Cys-Grx1 (upper panel) and ER-rxYFP (lower panel) from lysates of HGT1 cells incubated with 30 μM GSH for the indicated time, representative of those used to derive the data in E. **(E)** The ER glutathione redox potential ($E_{GSH.ER}$), and ER ratio of GSH/GSSG values used to derive the data in A–C. **(F)** Same as in A, but with 50 μM GSH. Values are the mean of three independent biological replicas ± standard deviation (s.d.).

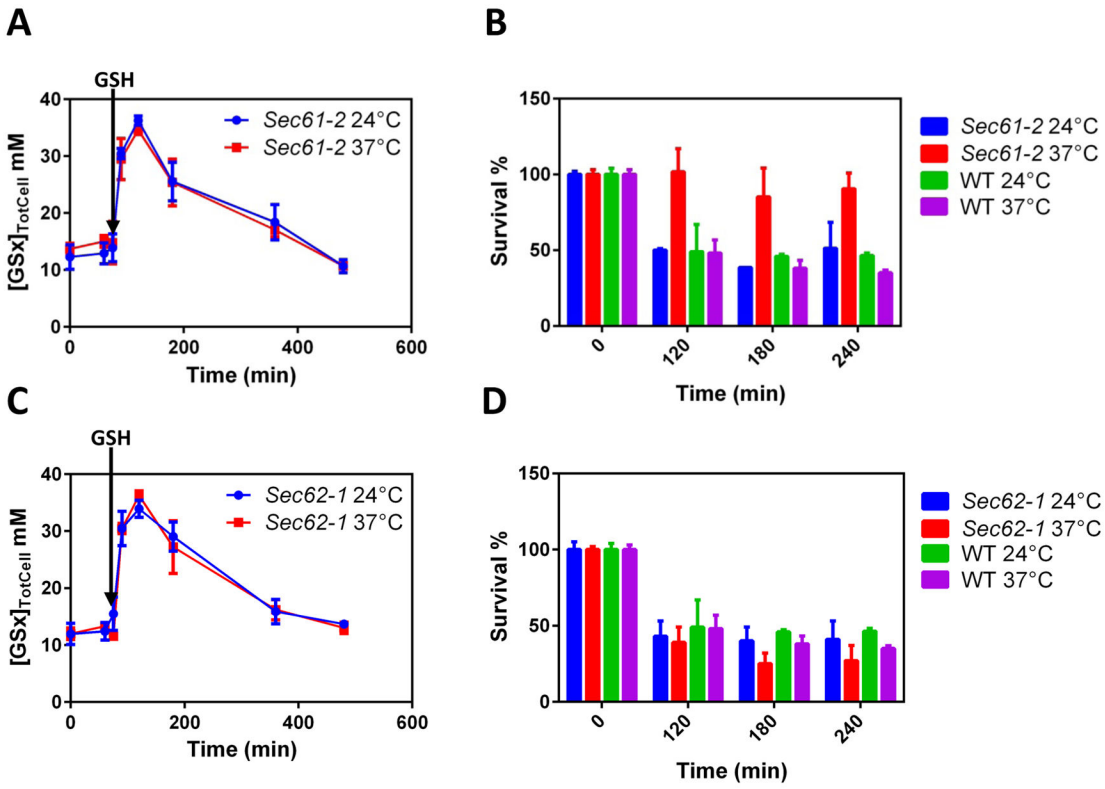


**Figure 3. A screen identifies the ER Sec61 protein-conducting channel as the ER GSH transporter**

**(A, C)** Total cellular levels (TotCell) of [GSx] in whole cell lysates of HGT1-*sec61-2* (A) or HGT1-*sec62-1* (C) cells. Cells were grown at 24 °C and then switched to 37 °C or left at 24 °C, as indicated, 45 min prior to GSH addition (30 μM) (arrow), and then incubated for the indicated time. **(B, D)** GSH survival assay. HGT1-*sec61-2* (B) or HGT1-*sec62-1* (D) cells were grown to the exponential phase at 24 °C, and switched to 37 °C or left at 24 °C, as indicated, 1 h prior adding GSH (30 μM), and then incubated for the indicated time. The survival rate is the % of colony forming units/number of cells at each time point. All values are the mean of three independent biological replicas ± standard deviation (s.d.).

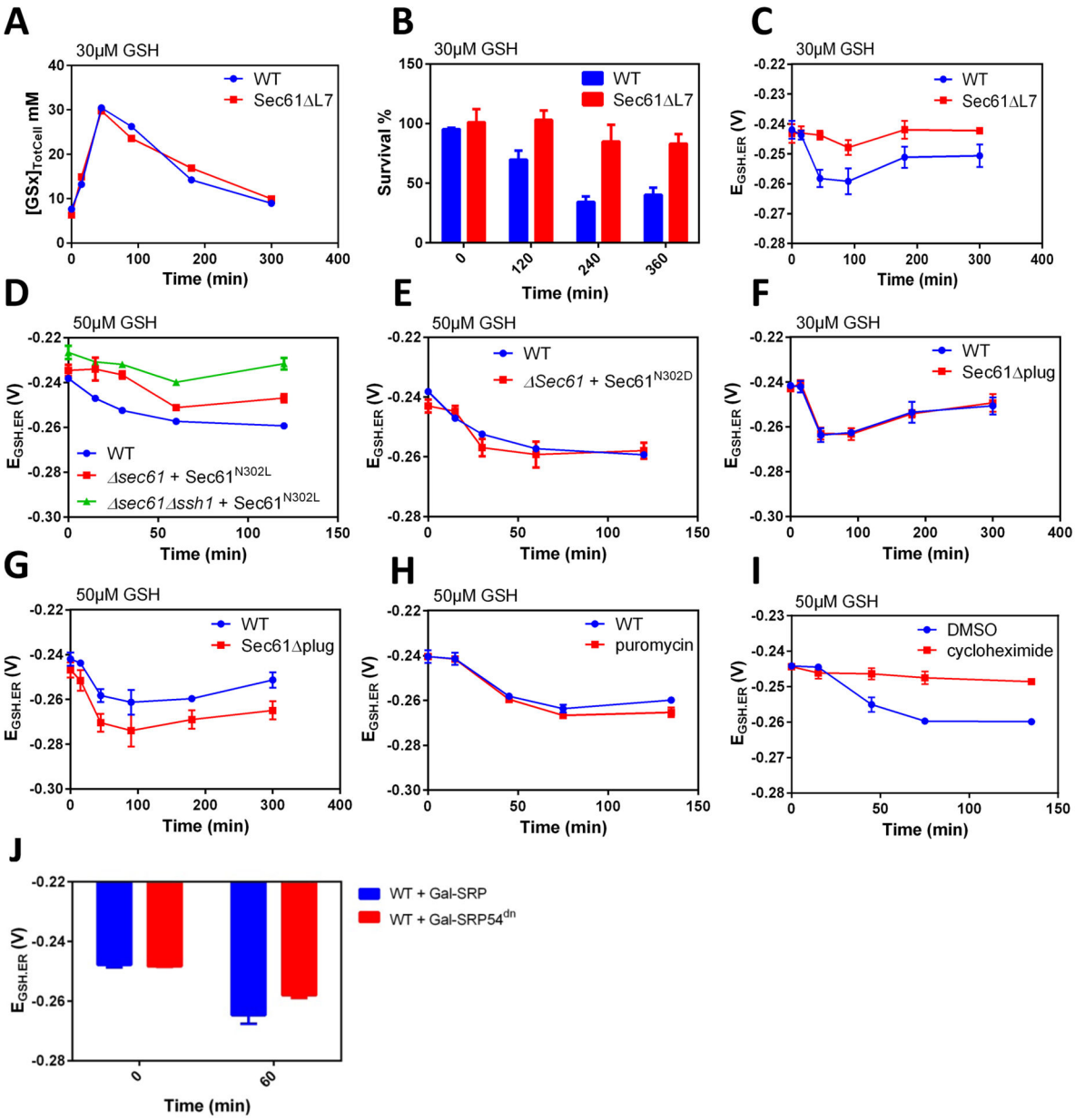


**Figure 4. Sec61 and Ssh1 serve in the ER transport of GSH**

**(A–C)** Total cellular levels (TotCell), survival rate (as in 3B, D), and $E_{GSH.ER}$ values in HGT1 and HGT1-Δ*sec61-sec61Δ7* cells incubated with 30 μM GSH for the indicated time. **(D–G)** $E_{GSH.ER}$ values in HGT1 cells (D–G), HGT1-Δ*sec61sec61N302L*, or HGT1-Δ*sec61*Δ*ssh1sec61N302L* as indicated (D), HGT1-Δ*sec61sec61N302D* (E), HGT1-Δ*sec61*Δplug (F, G), incubated during the indicated time with the indicated amount of GSH. **(H)** Value of $E_{GSH.ER}$ in HGT1-Δ*erg6*Δ*pdr1*Δ*pdr3* cells after incubation with 50 μM GSH during the indicated time. Puromycin (2 mM) was added 20 min prior to GSH addition. **(I)** Value of $E_{GSH.ER}$ in HGT1 cells after incubation with 50 μM GSH during the indicated time. Cycloheximide (CHX) (200 μg/mL) or vehicle (DMSO) was added 15 min prior to adding GSH. **(J)**. Value of $E_{GSH.ER}$ in HGT1 cells expressing *SRP54* or *SRP54*$^{dn}$ from a

*GAL1* promoter incubated 60 min with 30 μM GSH, 3 h after switching the medium from raffinose to galactose. All values are the mean of three independent biological replicas ± standard deviation (s.d.)

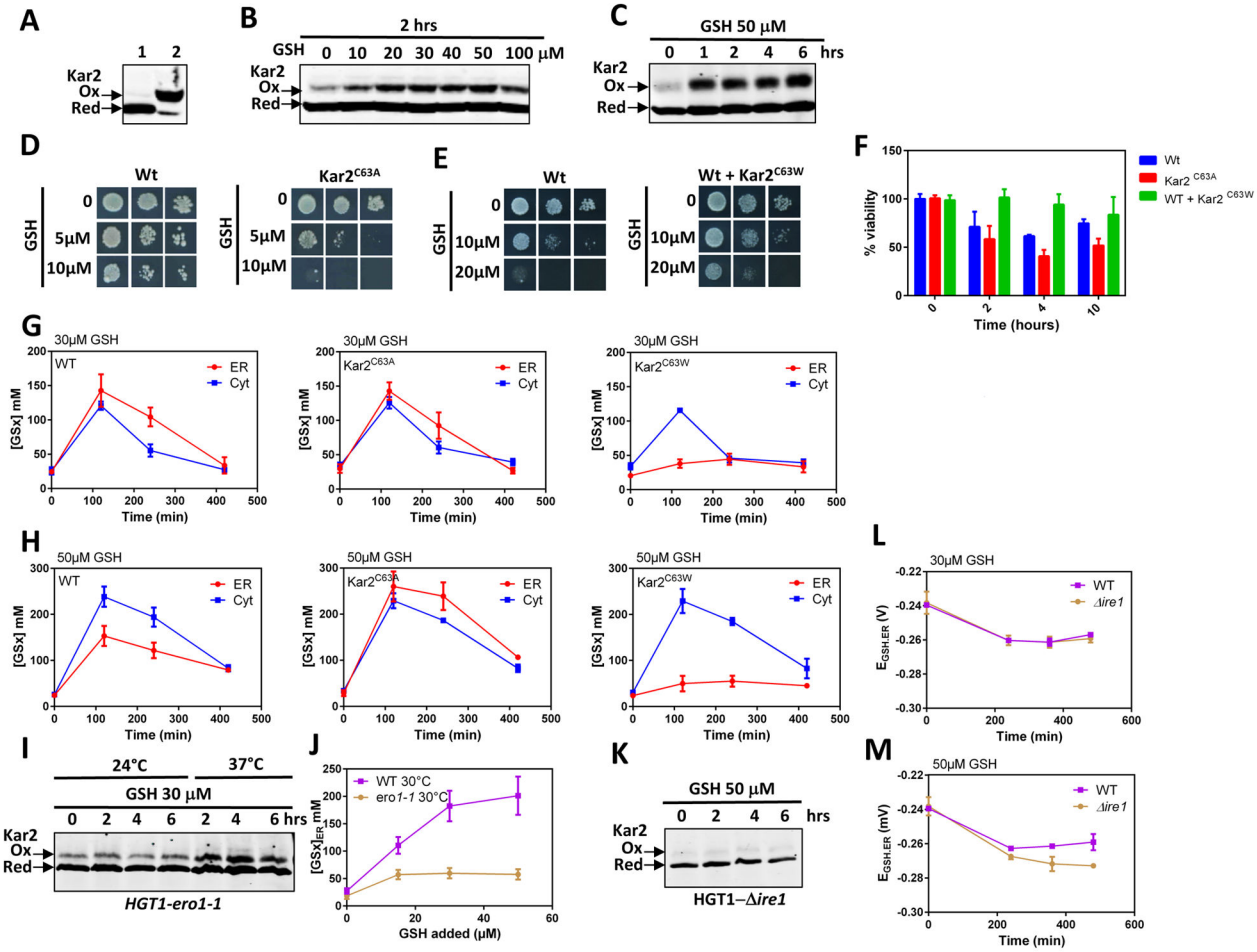


**Figure 5. Kar2 oxidation inhibits the ER transport of GSH**

**(A, B, C)** Kar2 redox westerns after SDS-PAGE migration. DTT-reduced samples alkylated by either NEM (lane 1) or PEG-maleimide (lane 2) served as control for reduced and oxidized Kar2 migration, respectively (A). Lysates of HGT1 cells incubated 2 h with the indicated amount of GSH, were alkylated with NEM, then reduced and alkylated with Mal-PEG-maleimide (B). Lysates of HGT1 cells incubated with 50 µM GSH during the time indicated and processed as in B. The 2, 4 and 6 h samples contain ½ the amount of lysate, relative to untreated (0 h) (C). Data representative of at least two experiments. **(D, E)** Tolerance to GSH by growth on plates containing the indicated amount of GSH. HGT1 cells (Wt) and HGT1-Δ*kar2* cells expressing $Kar2^{C63A}$ (D); HGT1 cells (Wt) expressing or not $Kar2^{C63W}$ (E). Data are representative of at least two experiments. **(F)** Survival rates to 50 µM GSH of the cells used in D and E, as indicated, assayed as in Figure 3B, D. **(G, H)** Corrected cytosolic (Cyt) (TotCell x 4.5) and ER (ER) levels of [GSx] after incubation with 30 µM (G) or 50 µM GSH (H) of the cells used in D and E, and during the time indicated. **(I)** HGT1-*ero1-1* cells incubated with 30 µM GSH at the temperature and time indicated were processed as in B and C for Kar2 oxidation. **(J)** ER $[GSx]_{ER}$ levels in HGT1 or HGT1-*ero1-1* cells, as indicated, incubated 2 h at 30 °C with the indicated amount of GSH. **(K)** HGT1-Δ*ire1* cells incubated with 50 µM GSH for the indicated time and processed for Kar2

oxidation as in B and C. **(L, M)** Values of $E_{GSH.ER}$ in HGT1 or HGT1-Δ*ire1* cells incubated with 30 (L) or 50 (M) μM GSH for the indicated time. Values in F–H, J, L, and M are the mean of three independent biological replicas ± standard deviation (s.d.).

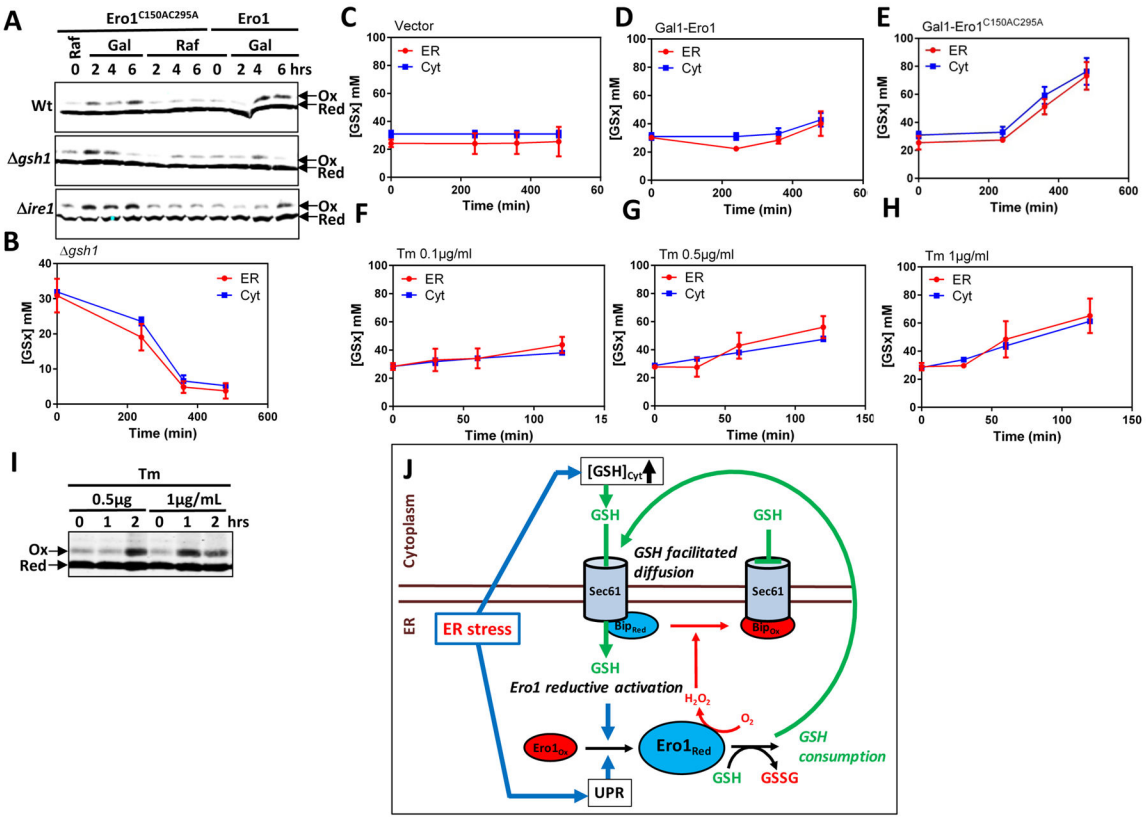


**Fig. 6. Reciprocal interplay between the ER import of GSH and Ero1 activation**

**(A)** Kar2 oxidation in Wt, Δ*gsh1*, and Δ*ire1* expressing Ero1$^{C150AC295A}$ or Ero1 from a *GAL1* promoter, as indicated, grown in raffinose or galactose medium for the indicated time and processed as in Figure 5B, C. **(B–H)** Corrected cytosolic (Cyt) (TotCell x 4.5) and ER (ER) [GSx] in Δ*gsh1* incubated during the indicated time in medium lacking GSH (B); in HGT1 cells carrying an empty vector (C), Gal1-*ERO1* (D), or Gal1-*ERO1*$^{C150AC295A}$ (E), switched from raffinose to galactose medium at time 0 (C–E); in Wt cells incubated with 0.1 (F), 0.5 (G) or 1 μg/mL (H) tunicamycin (Tm) for the indicated time (F–H). **(I)** Wt cells incubated with 0.5 or 1 μg/mL tunicamycin (Tm) for the indicated time were processed for Kar2 oxidation as in Figure 5B, C. The 1- and 2-h 0.5μg/ml Tm samples contain ½ and ¼ the lysates amount relative to untreated (0 h), respectively, and the 1- and 2-h 1 μg/mL samples ¼ and 1/6 relative to 0 h. Values in B–H are the mean of three independent biological replicas ± standard deviation (s.d.). **(J)** Proposed model. ER stress stimulates both $[GSH]_{Cyt}$ increase and UPR-dependent Ero1 *de novo* synthesis. $[GSH]_{Cyt}$ increase stimulates ER facilitated diffusion of GSH, which promotes Ero1 reductive activation, and further stimulates GSH import by GSH oxidation to GSSG. UPR-dependent Ero1 level increase is critical for allowing active Ero1-dependent $H_2O_2$ production to reach the threshold levels required to oxidize Kar2, which inhibits GSH import, in turn allowing Ero1 activity to cease.

**Table 1**

GSH parameters measured in exponentially growing Wt and Δ*glr1* cells.

| | | [GSx] (mM)[1] | [GSH] (mM) | [GSSG] (mM) | $E_{GSH}$ (mV) | [GSH]/[GSSG] |
|---|---|---|---|---|---|---|
| Wt | ER[2] | 30 ± 2 | 29.6 ± 2 | 0.60 ± 0.04 | −242 ± 2 | 42 ± 2 |
| | TotCell[3] | 7 ± 1 | 6.6 ± 1 | 0.40 ± 0.05 | −289[6] | NA[7] |
| | Cor.TotCell[4] | 31. 5 ± 4.5 | 29.7 ± 4.5 | NA[8] | −289[6] | NA |
| Δ*glr1* | ER[2] | 31 ± 1 | 29 ± 1 | 1.20 ± 0.03 | −235 ± 3 | 22 ± 2 |
| | Cytosol[5] | 31 ± 1 | 30 ± 1 | 0.50 ± 0.03 | −246 ± 2 | 46 ± 3 |
| | TotCell[3] | 7.14 ± 1 | 6.44 ± 1 | 0.40 ± 0.05 | NA | NA |
| | Cor.TotCell[4] | 32.13 ± 4.5 | 28.98 ± 4.5 | 1.80 ± 0.23 | NA | NA |

[1] [GSx] = [GSH] + 2[GSSG]

[2] Calculated from data obtained using ER-rxYFP and ER-1-Cys-Grx1

[3] Measured in total cell lysates by enzyme assay

[4] 4.5-fold corrected value of $[GSx]_{TotCell}$ (see text and supplemental Fig. S2).

[5] Calculated from data obtained using Cyt-rxYFP and Cyt-1-Cys-Grx1

[6] Established in (Ostergaard et al., 2004)

[7] Non applicable

[8] The correction cannot be applied to GSSG, as TotCell also contains the vacuolar GSSG